

## Four-dimensional Ising spin glass: scaling within the spin-glass phase

This article has been downloaded from IOPscience. Please scroll down to see the full text article.

1993 J. Phys. A: Math. Gen. 26 6731

(<http://iopscience.iop.org/0305-4470/26/23/021>)

View [the table of contents for this issue](#), or go to the [journal homepage](#) for more

Download details:

IP Address: 171.66.16.68

The article was downloaded on 01/06/2010 at 20:11

Please note that [terms and conditions apply](#).

# Four-dimensional Ising spin glass: scaling within the spin-glass phase

J C Ciria†, G Parisi‡ and F Ritort§

† Departamento de Física Teórica, Universidad de Zaragoza, Pza S Francisco s/n, 50009 Zaragoza, Spain

‡ Dipartimento di Fisica, Università di Roma I, 'La Sapienza', Piazzale Aldo Moro, Roma 00100, Italy and INFN, Sezione di Roma, 'Tor Vergata', Via della Ricerca Scientifica, Roma 00133, Italy

§ Dipartimento di Fisica, Università di Roma II, 'Tor Vergata', Via della Ricerca Scientifica, Roma 00133, Italy and Departament de Física Fonamental, Universitat de Barcelona, Diagonal 648, 08028 Barcelona, Spain

Received 5 January 1993

**Abstract.** We investigate the nature of the spin-glass phase in the four-dimensional Ising spin glass. We study the probability distributions of overlaps, of energy overlaps and ultrametricity for several sizes. We discover the existence of finite-size scaling in the tails of the first and second of these. This allows us to extract some exponents within the spin-glass phase. We also perform studies on quenched thermalization of large samples. Our results together with previous work favour the mean-field picture of the spin-glass phase.

## 1. Introduction

Our knowledge of spin-glass theory [1–3] is based mainly on two different approaches. The first, known as the replica approach, relies on the solution to the infinite-range model [4]. It predicts the nature of the spin-glass phase at finite dimensions (and above the lower critical dimension) similar to that known in the mean-field theory [5]. The second approach is based on the phenomenological theory of droplets [6] and predicts a spin-glass phase dominated by a unique state with a spectrum of excitations given by reversal of domains of spins (droplets). There are several reasons why four-dimensional spin glasses are of great interest from the standpoint of simulations [7]. Several works have addressed the question about what the nature of the spin-glass phase is in four-dimensional Ising spin glasses, these include studies of the overlap probability distribution [8] and others on the existence of a transition in a finite magnetic field [9, 10].

In this work we study the four-dimensional Ising spin glass at zero external magnetic field by means of Monte Carlo numerical simulation for several small sizes  $N = L^4$  with  $L = 3, 4, 5, 6$ . This work, a natural continuation of previous work, sheds new light on the nature of the spin-glass phase. Section 1 gives an overview of the features of the spin-glass phase expected within the mean-field picture. We predict the existence of some scaling laws within the spin-glass phase and recall some ideas which have already been presented [7]. Section 2 shows results for the overlap probability distribution, i.e.  $P(q)$ , and we find the existence of finite-size scaling laws. This gives support to the non-triviality of the  $P(q)$ . In section 3 we study the probability distribution for the overlap energy (first introduced in [11]). The existence of two singularities for  $P(q^e)$  gives further support to the mean-field

picture. Section 4 is devoted to ultrametricity and section 5 to some results on the dynamics of thermalization for large samples.

## 2. Finite-size scaling in the spin-glass phase

Recently it has been shown for the Sherrington–Kirkpatrick (SK) model that finite-size corrections to some quantities within the spin-glass phase can be computed analytically [14, 15]. It is possible that the mean-field description of the spin-glass phase survives below the upper critical dimension which is generally accepted to be six. Above six dimensions we expect to find mean-field behaviour. Theoretical [12] and numerical results† support this idea.

Generally speaking, the Ising spin-glass model is given by the hamiltonian

$$H = - \sum_{(i,j)} J_{ij} \sigma_i \sigma_j - h \sum_i \sigma_i \quad (1)$$

where the  $J_{ij}$  are quenched variables with zero mean. The sum runs over nearest neighbours. In case of the SK model all spins are connected among them and the variance of the  $J_{ij}$  goes like  $1/N$ . The overlap probability distribution  $P(q)$  is defined by

$$P(q) = \left\langle \delta \left( q - \frac{1}{N} \sum_i \sigma_i \tau_i \right) \right\rangle \quad (2)$$

where  $\{\sigma_i, \tau_i\}$  are the spins of two independent replicas,  $\langle (\cdot) \rangle$  means thermodynamic average and  $\overline{(\cdot)}$  means average over samples.

Our present knowledge of the SK model is good even though there are some problems as yet unresolved, particularly in the behaviour of finite-size corrections for the thermodynamic potentials within the spin-glass phase [14]. Nevertheless, quite recently it has been shown that some finite-size corrections within the spin-glass phase can be computed analytically. One of these predictions concerns the finite-size behaviour of the tail of the  $P(q)$  when the size  $N$  increases. It has been shown [14, 15] that

$$P(q > q_{\max}) \sim N^{1/3} \exp(-aN(q - q_{\max})^3) \quad (3)$$

where  $N$  is the size of the system,  $a$  is a constant and  $q_{\max} = q(1)$  is the maximum overlap (taken at the thermodynamic limit).

This result comes naturally from the behaviour of the Gaussian propagators in the mean-field theory below the critical temperature as derived in [16]. It would be very interesting to find some scaling of this type in finite-dimensional spin glasses below six dimensions. Within the replica theory approach one expects that soft modes will survive at finite dimensions even though it should be clear what the form of the exact propagators is within the spin-glass phase [17]. The soft modes are the signature of a divergence and in the mean-field theory they are the origin of the non-Gaussian behaviour of the tail of the  $P(q)$ . The study of the tail of the  $P(q)$  should allow us to study questions about its triviality and what the parameters which characterize the peak of the  $P(q)$  are, i.e. the nature of the singularity and the value of  $q(1)$ . On the other hand, one can investigate the criticality of

† We have received a preprint by J Wang and A P Young in which they study numerically the spin glass at six dimensions. Their results show mean-field behaviour with logarithmic corrections at the critical point.

the spin-glass phase [12] and make precise predictions that a future spin-glass field theory should reproduce.

The existence of this scaling has a parallel that has been presented in a recent work [7]. Let us recall the main ideas and how one can define some critical exponents within the spin-glass phase. Suppose we couple two identical replicas with a field  $\epsilon q$  [13]:

$$H_1 = - \sum_{(i,j)} J_{ij} \sigma_i \sigma_j - \sum_{(i,j)} J_{ij} \tau_i \tau_j - \epsilon \sum_i \sigma_i \tau_i \tag{4}$$

where the sum  $(i, j)$  runs over the nearest neighbours in a lattice of  $D$  dimensions and the  $J_{ij}$  are quenched random variables.

A finite discontinuity in the overlap  $q(\epsilon)$  is expected as  $\epsilon \rightarrow 0$ . It is defined as

$$\delta q = \lim_{\epsilon \rightarrow 0^+} (q(\epsilon) - q(-\epsilon)) = 2q_{\max}. \tag{5}$$

It is expected that

$$q(\epsilon) = q(0^+) + C_+ \epsilon^{\omega_{qq}} \tag{6}$$

where  $\omega_{qq} = dq/(D - dq)$  as defined in [7].  $dq$  are the dimensions of the operator  $Q_{ab}$  (which above six dimensions are half the dimensions of the operator energy). In some sense, the spin glass is always critical in the whole low-temperature region [18] where behaviour similar to equation (6) is expected also at the critical temperature where, in terms of the critical exponents  $\beta, \nu, \eta$ , the exponent  $dq$  is given by

$$dq = \frac{\beta}{\nu} = \frac{D - 2 + \eta}{2}. \tag{7}$$

Because of the existence of soft modes within the spin-glass phase (in fact the nonlinear susceptibility and the correlation length of the  $q$ - $q$  correlation function diverge within the spin-glass phase) we expect that these definitions of the critical exponents will work also within the spin-glass phase (even though the values of the exponents could differ from those at the critical point).

As a consequence of these results the tail of the  $P(q)$  is expected to behave as

$$P(q > q_{\max}) \sim P_{\max} f(N(q - q_{\max})^{D/dq}) \tag{8}$$

where  $N = L^D$  is the size of the system,  $P_{\max}$  is the height of the peak of the  $P(q)$  and  $q_{\max}$  is the position of the singularity of  $P(q)$  in the infinite-size limit. If  $z = N(q - q_{\max})^{D/dq} \gg 1$  we expect that  $f(z) \sim \exp(-Az)$ .

*A priori* we cannot say how  $P_{\max}$  behaves with size. It depends on the type of singularity of  $P(q)$  at  $q = q_{\max}$ . If the singularity is of the delta type we expect that  $P_{\max} \sim L^{dq}$ . For example, in mean-field theory  $P_{\max} \sim L^2$  and  $dq = 2$  since the singularity is of the delta type.

With the Hamiltonian (4) one can expect that for  $q > q_{\max}$

$$P(q > q_{\max}) \sim \exp[-(AN(q - q_{\max})^{D/dq} + \beta N \epsilon q)] \tag{9}$$

where  $\beta$  is the inverse of the temperature. The maximum contribution to the saddlepoint equation (9) gives  $q(\epsilon)$ . Comparing this result with (6) we obtain

$$C_+ = \left( \frac{dq\beta}{AD} \right)^{dq/D-dq} \tag{10}$$

This result connects both predictions (6) and (8) quantitatively. It shows that the study of the tail of the  $P(q)$  for  $q > q_{\max}$  is equivalent to the behaviour of  $q(\epsilon)$  for  $\epsilon \rightarrow 0^+$  when two replicas are coupled as in the Hamiltonian (4).

The same observations are valid for the energy overlap introduced in [11] to study the three-dimensional Ising spin glass. It is defined as

$$q^e = \frac{1}{8N} \sum_{(i,j)} J_{ij}^2 \sigma_i \sigma_j \tau_i \tau_j \quad (11)$$

where the sum  $(i, j)$  runs over nearest neighbours. In our numerical simulations  $J_{ij} = \pm 1$  and  $J_{ij}^2 = 1$ .

Coupling two replicas  $\sigma, \tau$  with a field  $\epsilon q^e$  we are led to the following Hamiltonian:

$$H_2 = - \sum_{(i,j)} J_{ij} \sigma_i \sigma_j - \sum_{(i,j)} J_{ij} \tau_i \tau_j - \epsilon \sum_{(i,j)} \sigma_i \tau_i \sigma_j \tau_j. \quad (12)$$

When the coupling  $\epsilon$  is different from zero the system selects the maximum or the minimum overlap  $q^e$  according to the sign of  $\epsilon$ . One can define the energy overlap probability distribution  $P(q^e)$ :

$$P(q^e) = \overline{\{\delta(q - q^e)\}} \quad (13)$$

If  $P(q^e)$  has a finite support in the infinite-size limit for  $\epsilon = 0$  then we expect that there will be a finite discontinuity in  $q^e(\epsilon)$  as  $\epsilon$  goes to zero from the positive or the negative side. As in the case of the overlap  $q$ , the discontinuity in  $q^e$  is defined as  $\delta q^e = q^e(0^+) - q^e(0^-)$ . The existence of a discontinuity in  $q^e$  within the spin-glass phase is very important since it shows the existence of at least two thermodynamic states which are not related by inversion of compact domains.

In infinite dimensions (SK model) one has  $q^e = q^2$ . This means that  $q^e(0^-) = 0$ . This is not the case at finite dimensions, where it has been shown previously that  $q_e(0^-)$  is finite (we have seen it at four and six dimensions). As we will see in section 3, the existence of a continuous part in  $P(q^e)$  is an indication of the existence of several thermodynamic states as predicted within mean-field theory. Similarly, as we showed in equation (8), we expect that  $P(q^e)$  will present two peaks at  $q_{\min}^e = q^e(0^-)$  and  $q_{\max}^e = q^e(0^+)$  with two respective tails. For example, the right tail of the  $P(q^e)$  will show the following scaling behaviour:

$$P(q^e > q_{\max}^e) \sim P_{\max}^e \exp(-B_+ N (q^e - q_{\max}^e)^{D/de}). \quad (14)$$

Introducing a coupling  $\epsilon > 0$  according to equation (4) we expect that

$$q^e(\epsilon_e) = q^e(0^+) + E_+ \epsilon^{\omega_{ee}} \quad (15)$$

with  $\omega_{ee} = de/(D - de)$  where  $de$  has dimensions of the operator energy. At the critical point the exponent  $\omega_{ee}$  is given by the critical exponents  $\alpha$  and  $\nu$  through  $de$ :

$$de = 1 - \frac{\alpha}{\nu}. \quad (16)$$

Since  $\omega_{ee} > 1$  at the critical point then equation (15) will be dominated by the regular terms and  $\omega_{ee} = 1$ . Also, in this case both approaches (tail of  $P(q_e)$  and study of  $q^e(\epsilon)$ ) are equivalent. The constants  $E_+$  and  $B_+$  are related by

$$E_+ = \left( \frac{de\beta}{B_+ D} \right)^{de/(D-de)} \quad (17)$$

The same is expected for  $P(q^e < q_{\min}^e)$ .

In order to finish this introduction and to test these ideas we show some numerical results for the SK model which is under control.

We have studied the SK model with binary couplings at  $T = 0.5$  (half the critical temperature) for  $N = 2080$  (this is a very large size which we can simulate in a reasonable amount of computer time). Figure 1 shows data for  $q(\epsilon)$  for  $\epsilon$  positive. Since  $\omega_{qq} = 1/2$  in mean-field theory then it is plotted versus  $\epsilon^{1/2}$ . The system thermalizes very fast for  $\epsilon$  not too small. Fitting the data to equation (6) with  $\omega_{qq} = 1/2$  and a regular term proportional to  $\epsilon$  we obtain  $C_+ = 1.1$  and  $q_{\max} = 0.6$ . In order not to have saturation effects because  $q$  is close to one, we can fit the local field  $h_q = \tanh^{-1}(q)$ . Data are shown in figure 2. In this case we obtain  $C_+ = 1.2$  and  $q_{\max} = 0.59$ , which are consistent with the previous values. The value of  $q_{\max}$  is in good agreement with that found at first order of replica symmetry breaking ( $q_{\max} \simeq 0.6125$ ). These values obtained for  $C_+$  and  $q_{\max}$  are only approximate and we should go to larger sizes and smaller values of  $\epsilon$  in order to obtain more precise results. From the value of  $C_+$  obtained from fitting  $q$  and using equation (10) we obtain  $A = 0.6$  and we expect that the tail of  $P(q)$  scales like

$$P(q > q_{\max}) \sim N^{1/3} \exp(-0.6N(q - 0.60)^3). \tag{18}$$

Our data for several tails of the  $P(q)$  corresponding to different sizes ranging from  $N = 32$  up to  $N = 768$  are shown in figure 3. They are plotted on a logarithmic vertical scale and the continuous line is a good fit to our data

$$P(q > q_{\max}) \sim N^{1/3} \exp(-0.8N(q - 0.62)^3). \tag{19}$$

This is very similar (within error bars) to equation (18) predicted from the analysis of the coupling of two replicas. One comment on figure 3 is in order. In fact, the data seem to display a small curvature. This is because when exponential behaviour of equation (19) is expected for  $N(q - 0.62)^3 \gg 1$ , i.e. the tail is far from the maximum. Since our data on the  $x$  axis of figure 3 range only up to five it is not strange to find the existence of a slight curvature. We now present our results on the four-dimensional Ising spin glass.

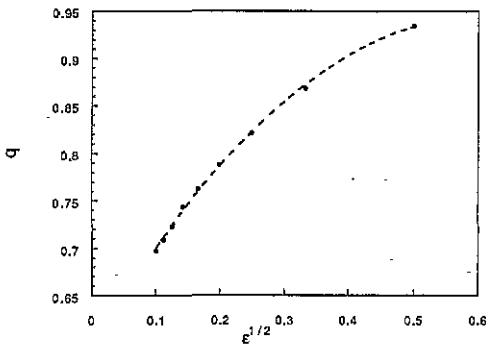


Figure 1.  $q(\epsilon)$  versus  $\epsilon^{1/2}$  in the SK model with  $N = 2080$  at  $T = 0.5$ . A two-degree polynomial fit to the data gives  $q_{\max} = 0.6$  and  $C_+ = 1.1$ .

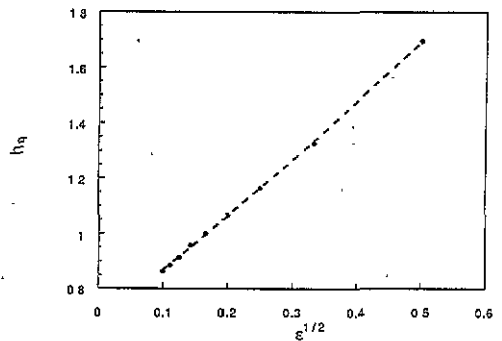
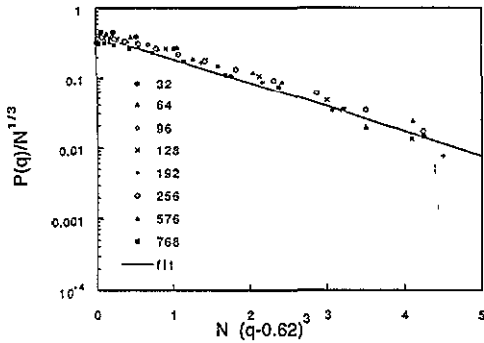
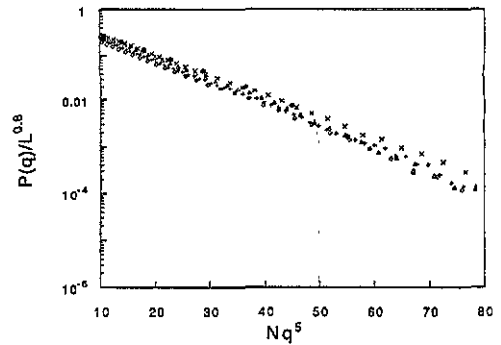


Figure 2.  $h_q$  versus  $\epsilon^{1/2}$  in the SK model with  $N = 2080$  at  $T = 0.5$ .



**Figure 3.** Tails of  $P(q)/N^{1/3}$  in the SK model versus  $N(q - 0.62)^3$  for several sizes  $N = 32-768$  at  $T = 0.5$ . The straight line is the approximate fit using equation (19).



**Figure 4.**  $P(q)/L^{0.8}$  very near to the critical point at  $T = 2.0$  in the four-dimensional case.  $\bullet$ ,  $L = 3$ ;  $\Delta$ ,  $L = 4$ ;  $\diamond$ ,  $L = 5$ ;  $\times$ ,  $L = 6$ ;  $+$ ,  $L = 7$ .

### 3. Numerical results for the $P(q)$

We have studied the four-dimensional Ising spin glass equation (1) ( $J_{ij} = \pm 1$ ) for several sizes  $L = 3, 4, 5$  and 6 and 64 samples in each case. In one case we were also able to simulate  $L = 7$ . We simulated eight different replicas evolving in parallel for each sample. Since the main problem of these simulations is the thermalization within the spin-glass phase we have made use of a simulated annealing procedure in order to ensure full equilibration. For sizes  $L = 3, 4, 5$  this is relatively easy to achieve, at least for temperatures that are not too low ( $T > T_c/2$ ). For  $L = 6$  and 7 we have been able to thermalize the samples down to  $T = 0.77T_c$  and  $T = 0.75T_c$  respectively; the thermalization time grows enormously as the temperature is progressively decreased. Knowing that  $T_c \simeq 2.02 \pm 0.03$  [10, 20] we decreased the temperature from  $T = 3$  down to  $T = 1$  at constant steps of  $\Delta T = 0.2$ . At each step we performed a minimal number of Monte Carlo steps  $nt$  in order to thermalize the system. This number  $nt$  grew as the temperature decreased. We found that a power-law increase of  $nt$  with the  $k$ -step during annealing ensured good thermalization. Statistics were collected over 20 000 Monte Carlo steps. As already noted, for  $L = 6$  we were able to thermalize only down to  $T = 1.4$  and down to  $T = 1.5$  for  $L = 7$ .

We begin by showing our results very close to the critical point. Figure 4 shows the finite-size scaling law equation (8) at  $T = 2.0$ . Even though this is not exactly the critical point we expect that critical effects will dominate the behaviour (at least for the small sizes we have studied). In this case  $P_{\max} \sim L^{dq}$  and we obtain  $\omega_{qq} \simeq 0.25$  in agreement with previous studies. In fact, and this comment is valid for the rest of the work, it is difficult to estimate errors for our fits. Our results are thus approximate and their precise determination would require more intensive work (more samples and more statistics).

We now move within the spin-glass phase far from the critical point. Figure 5 shows the  $P(q)$  for several sizes at  $T = 1.5$ . We can see the typical features of mean-field theory for the  $P(q)$ —a peak whose height grows and whose position on the  $q$ -axis moves towards smaller values of  $q$  as size increases. Figure 6 shows the finite-size scaling of the tail of the  $P(q)$ . We plot  $P(q)/P_{\max}$  versus  $N(q - q_{\max})^{D/dq}$  on a logarithmic vertical scale. Our best fit to equation (8) gives  $dq = 0.88$ ,  $q_{\max} = 0.43$ . All tails seem to fall on the same straight line. Our prediction for  $\omega_{qq} \simeq 0.28$  is compatible with the results obtained by fitting equation (6),  $\omega_{qq} \simeq 0.3-0.4$  [7].

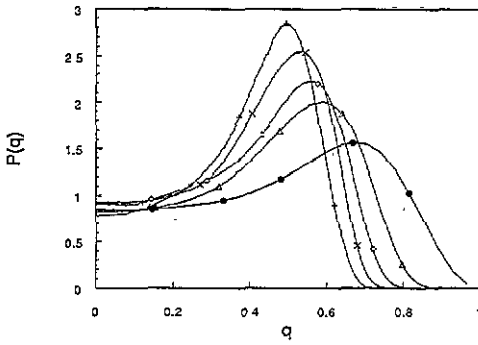


Figure 5.  $P(q)$  at  $T = 1.5$  in the four-dimensional case for several sizes. ●,  $L = 3$ ; △,  $L = 4$ ; ◇,  $L = 5$ ; ×,  $L = 6$ ; +,  $L = 7$ .

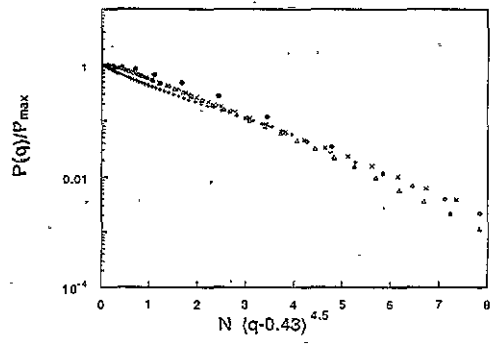


Figure 6. Tails of  $P(q)/P_{\max}$  at  $T = 1.5$  in the four-dimensional case. The same symbols as in figure 5.

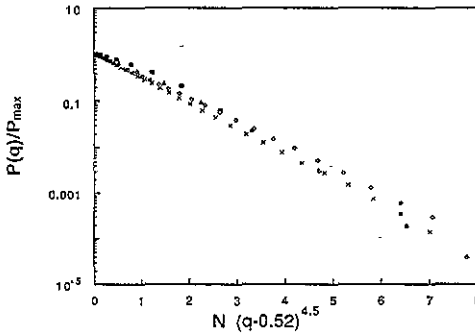


Figure 7. Tails of  $P(q)/P_{\max}$  at  $T = 1.4$  in the four-dimensional case for several sizes. ●,  $L = 3$ ; △,  $L = 4$ ; ◇,  $L = 5$ ; ×,  $L = 6$ .

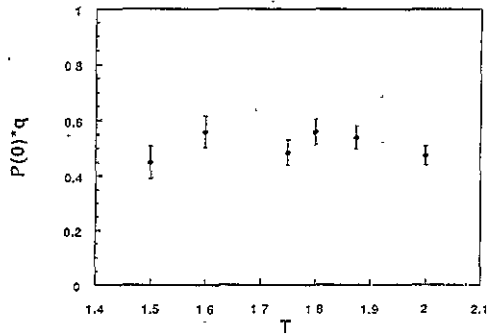


Figure 8. The product  $P(0)q_{\max}$  at several temperatures from  $T = 1.875$  down to  $T = 1.5$  for  $L = 6$ .

Figure 7 shows data on the tails of the  $P(q)$  at a slightly lower temperature  $T = 1.4$ . In this case our best fit gives  $q_{\max} = 0.54$ ,  $dq = 0.88$ . It would be very interesting to establish more clearly what the values of the exponents  $dq$  and  $\omega_{qq}$  are in the low-temperature phase. In mean-field theory they take the same values as at the critical point, but this may not be true in finite dimensions. We cannot decide on this point due to the low precision of our data (few samples and small sizes).

Another interesting question refers to the increase of  $P_{\max}$  with size. To establish clearly how the height of the peak of the  $P(q)$  increases with size we would need more statistics and several more sizes. In any case, all our results are compatible with a delta-type singularity but more extensive numerical investigations of this point are required in order to confirm it.

We have also tested an interesting prediction of replica-field theory concerning the study of short-range corrections below six dimensions. Here it has been argued [21], using renormalization group arguments, that the scaling of the order parameter function is restored. This means that

$$q(x) = \tau^\beta f(x) \tag{20}$$

where  $\tau = (T_c - T)/T_c$ . As a consequence of this, taking into account the relation



$P(q) = dx/dq$  and  $q_{\max} \sim \tau^\beta$ , we obtain that the product  $P(0)q_{\max}$  should be constant below and near  $T_c$  (also one could use  $\langle q^2 \rangle^{1/2}$  instead of  $q_{\max}$ ). Data are shown in figure 8 for  $L = 6$  at five different temperatures from  $T = 2.0$  down to  $T = 1.5$ . This prediction is in agreement with our data.

#### 4. Numerical results for the $P(q^e)$

As we said in the introduction, the probability distribution for the energy overlap can also shed light on the nature of the spin-glass phase.

In figure 9 we show the  $P(q^e)$  for  $L = 3, 4, 5, 6$  at the critical point  $T = 2.0$ . The same comment we made in the last section for the  $P(q)$  applies here (we are not exactly at the critical point but we expect that critical effects will dominate).  $P(q^e)$  is strongly peaked at  $q^e \simeq 0.22$ . A finite-size scaling analysis according to equation (14) for the  $P(q^e)$  gives  $q_{\max}^e = q_{\min}^e = 0.225$  and  $de = 2$ . Figure 10 shows the finite-size scaling for the right part of the tail (the left part is very similar except that the value of  $B_-$  is different to  $B_+$ ). The value of  $dq$  shows that the scaling behaviour of  $P(q^e)$  is dominated by the regular terms ( $\omega_{ee} = 1$ ). In contrast to what happens in infinite dimensions,  $q_{\min}^e$  is different from zero. We expect it will be affected by  $1/D$  corrections and will only vanish in the case of the SK model.

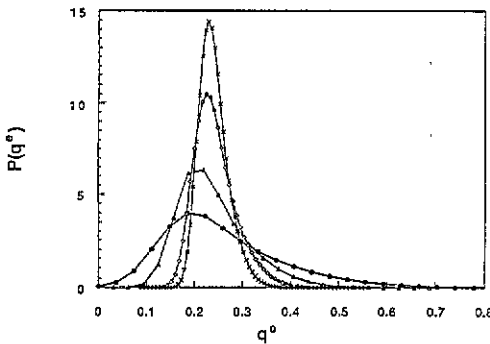


Figure 9.  $P(q^e)$  at  $T = 2.0$  in the four-dimensional case for several sizes.  $\bullet$ ,  $L = 3$ ;  $\Delta$ ,  $L = 4$ ;  $\diamond$ ,  $L = 5$ ;  $\times$ ,  $L = 6$ . There is a strong peak around  $q_{\max} = 0.22$ .

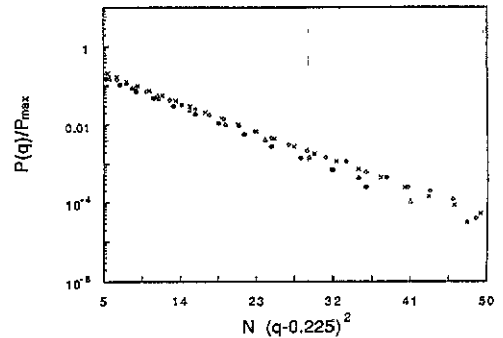


Figure 10. Right tail of the  $P(q^e)/P_{\max}^e$  at  $T = 2.0$  in the four-dimensional case for several sizes. Symbols as in figure 9.

Within the spin-glass phase we find that  $P(q^e)$  develops two peaks whose heights grow as the temperature is decreased. Figure 11 shows  $P(q^e)$  at  $T = 1.4$ . There are two peaks a finite distance apart. One comment on the  $P(q^e)$  shown in figure 11 is in order. Once we have thermalized our samples we compute  $P(q^e)$  over 20 000 Monte Carlo steps. At each Monte Carlo step we compute the  $P(q^e)$  over ten different overlaps  $q^e$  among the eight different replicas which evolve in parallel. Since the characteristic time in which the system passes from one thermodynamic state to another grows very rapidly when the size increases, then it becomes enormous particularly below the critical temperature. Because of this, 20 000 steps of statistics are not enough to go over all different states and during this time some of the eight replicas can become trapped in some wells. This explains why the height of the right peak of  $P(q^e)$  corresponding to  $q^e = q_{\max}^e$  in the case  $L = 6$  has decreased with respect to the same peak for  $L = 5$ . This statistical effect is not dangerous

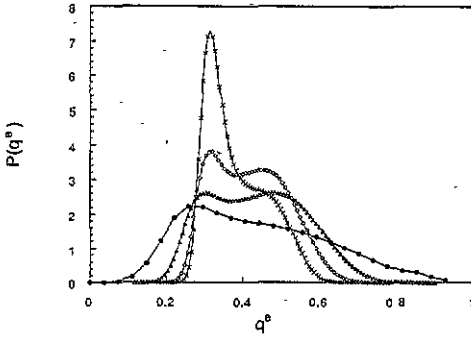


Figure 11.  $P(q^e)$  at  $T = 1.4$  in the four-dimensional case for several sizes. Symbols as in figure 9.

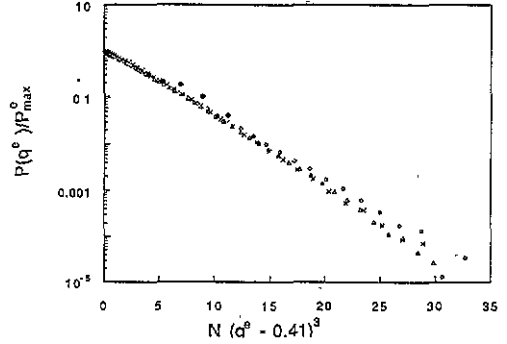


Figure 12. Right tail of the  $P(q^e)$  at  $T = 1.4$  in the four-dimensional case for several sizes. Symbols as in figure 9. The value of  $de$  is close to  $4/3$ .

when testing the scaling law (14) since only the quotient  $P(q^e)/P_{\max}^e$  enters in it and we hope that it will not be affected very much (and we have seen that this really is the case). This effect is also present in the case of the  $P(q)$  and we have bypassed it by normalizing the tail of the  $P(q)$  to its maximum height  $P_{\max}$ .

Figures 12 and 13 show our best fits to the right and left tails of the  $P(q^e)$ , respectively. We obtain  $de \simeq 1.33$  ( $\omega_{ee} = 1/2$ ) and  $q_{\max}^e = 0.41$ ,  $q_{\min}^e = 0.34$  and a finite discontinuity in the infinite-size limit  $\delta q^e \simeq 0.07$ . The value of  $de$  for the left tail is slightly greater than 1.33, but compatible with  $4/3$  by adjusting  $q_{\min}$ .

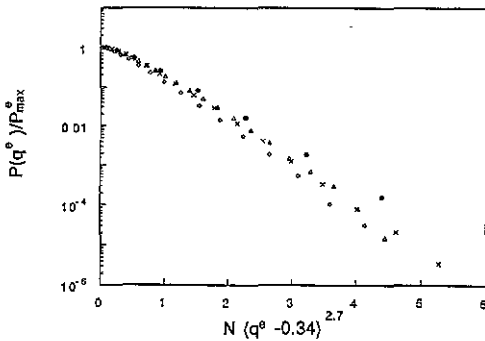


Figure 13. Left tail of the  $P(q^e)$  at  $T = 1.4$  in the four-dimensional case for several sizes. Symbols as in figure 9.

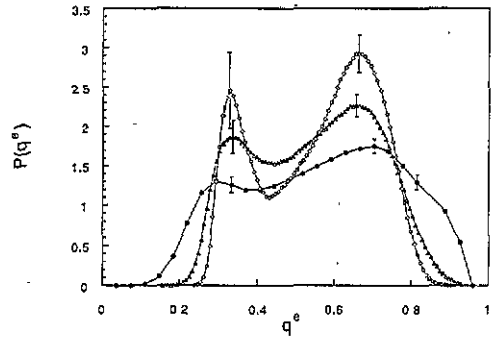


Figure 14.  $P(q)$  at  $T = 1.0$  in the four-dimensional case for three sizes.  $\bullet$ ,  $L = 3$ ;  $\Delta$ ,  $L = 4$ ;  $\diamond$ ,  $L = 5$ .

When the temperature is lowered we are only able to thermalize samples up to size  $L = 5$ . Figure 14 shows our results at  $T = 1$  and we find a great distance between the two peaks. In the plot we show some error bars because of the finite number of samples. One should be careful because, as we pointed out before, the error bars due to the finite number of statistics could be larger. The fact that the discontinuity  $\delta q^e$  is seen only at low temperatures proves that it increases below  $T_c$  with an exponent higher than that of the overlap  $q$ . Since  $\delta q^e \sim \tau^{vde}$  this is in agreement with the fact that  $de > 2dq$ .

## 5. Ultrametricity

Ultrametricity gives further information on replica symmetry breaking. It is not clear to us why ultrametricity should survive at finite dimensions even though replica symmetry is broken. In order to clarify this issue we have studied ultrametricity in the four-dimensional Ising spin glass. Our working temperature was  $T = 1.4$ . We chose this temperature because it is the highest one at which we are able to thermalize all the sizes and because at higher temperatures much precision and a very large number of samples are needed to see this effect clearly (this is also true for the SK model).

For each triad of three overlaps which we can compute among three different replicas we have analysed the difference between the middle one and the minimum when the maximum is less than 0.4 from the maximum overlap in the infinite-size limit ( $q_{\max} = 0.52$ ) as we estimated from our finite-size scaling for the  $P(q)$  (see figure 7).

Since ultrametricity is defined for states and not configurations of spins one has to be sure that finite-size corrections to the violation of the triangular inequality have been excluded. To this end, for each overlap  $q_{\alpha\beta}$  (which is the overlap among the configurations of spins) we found the distance between states  $\alpha$  and  $\beta$  which is given by

$$d_{\alpha\beta} = (2(q_{\max} - q_{\alpha\beta}))^{1/2} \quad (21)$$

where  $q_{\max}$  is the maximum overlap in the infinite-size limit. Only those triads of overlaps that satisfied the triangular inequality

$$d_{\max} \leq d_{\min} + d_{\text{med}} \quad (22)$$

were considered. In this way, finite-size corrections to the violation of ultrametricity which could also behave like  $\exp(-N(\delta q)^a)$  with  $\delta q = q_{\text{med}} - q_{\min}$  are excluded. Figure 15 shows our results for  $L = 3, 4, 5, 6$ . As we can see, the data are not very dependent on size. In fact, comparing with simulations done using the SK model or the hypercube model [22] at a similar temperature ( $T = 0.7T_c$ ), we would need more samples and statistics to decide this question or, better, to test the ultrametricity at lower temperatures.

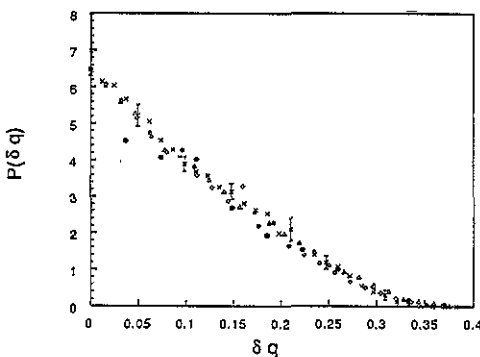


Figure 15. Ultrametricity at  $T = 1.4$ .  $\bullet$ ,  $L = 3$ ;  $\Delta$ ,  $L = 4$ ;  $\diamond$ ,  $L = 5$ ;  $\times$ ,  $L = 6$ . Some indicative error bars are shown for  $L = 6$ .

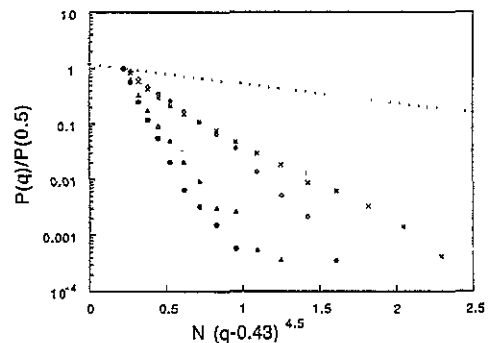


Figure 16. Tails of  $P(q)$  ( $T = 1.5, L = 14$ ) for  $q > q_0 = 0.5$  for different thermalization times  $t_0$  as described in the text.  $\bullet$ ,  $t_0 = 5000$ ;  $\Delta$ ,  $t_0 = 10000$ ;  $\diamond$ ,  $t_0 = 25000$ ;  $\times$ ,  $t_0 = 50000$ . The broken line is the numerical prediction equation (23) with  $a = 1.2$ ,  $b = 0.8$ .

## 6. Thermalization of large samples

In this final section we present some results on large samples and a more stringent test of our results on the finite-size scaling laws for small samples. In fact we have been able to establish with reasonable precision the value of the maximum overlap  $q_{\max}$  at several temperatures. Now we would like to stress our predictions by studying larger samples.

The main problem here is the thermalization. Nevertheless, we are able to obtain a lot of information by studying evolution of the  $P(q)$  after quenching from infinite temperature. Suppose that we want to establish  $q_{\max}$  for a very large size. By quenching the sample from infinite temperature it is probable that we would not be able to see the emergence of the singularity of the  $P(q)$  at  $q = q_{\max}$  in a reasonable amount of computer time. Since the peak of the  $P(q)$  measures the order parameter within one state (the Edwards–Anderson order parameter) and it is the part of the  $P(q)$  which thermalizes faster, it is logical to quench the samples from a strongly correlated configuration (for example all spins equal to 1 in all replicas) in order to reach the singularity before the region of large overlaps. The problem is that the overlaps go rapidly to zero and the samples decorrelate very fast.

To avoid this problem one can introduce in the Hamiltonian (1) a term of the type  $-\lambda\theta(q - q_0)$  with  $\lambda$  very great,  $\theta$  the Heaviside function and  $q_0$  an overlap greater than  $q_{\max}$ . In this way the system thermalizes with the constraint  $q > q_0$  and we can study the thermalization of the tail which is the part of the  $P(q)$  which does it most rapidly. To this end we have studied a large size ( $L = 14$ ) and we have quenched it from a configuration in which all spins were pointing up down to  $T = 1.5$  with  $q_0 = 0.5$ . We studied one sample and we looked at the evolution of the tail at four different thermalization times  $t_0 = 5000, 10\,000, 25\,000, 50\,000$  and statistics for the  $P(q)$  were collected over 2000, 5000, 5000 and 10000 Monte Carlo steps, respectively. Figure 16 shows our data for the tails  $P(q > q_0)$  normalized to  $P(q_0)$  versus  $N(q - 0.43)^{4.5}$  which is our numerical prediction and is shown as a broken line. We have fitted all four tails to an exponential of the type

$$P(q) = a \exp(-bN(q - 0.43)^{4.5}). \quad (23)$$

As  $t_0$  increases  $a$  takes the values 6.8, 3.8, 4.4 and 1.6. The correct value (broken line) is 1.2. The fitted values of  $b$  are 10.3, 7.9, 5.44, 3.55 while the predicted one in the infinite-time limit is 0.8. Then we expect that as the time increases the tails approach the predicted behaviour and this is the trend of our results. The approach is very slow (we expect that the equilibration time for the tail will behave like  $L^z$ ,  $z$  being a dynamical exponent and 50000 Monte Carlo steps are not too much) but we cannot conclude if they really converge to the numerical prediction and there could be some corrections to our fits of the tails of the  $P(q)$ .

Another way to proceed in order to study the tail of the  $P(q)$  is to quench two replicas from infinite temperature down to the temperature of interest during a number  $t_0$  of Monte Carlo steps. Then we expect the system will have thermalized over energy barriers of size  $T \log(t)$ . After that, we put the two configurations of both replicas equal to each other and study the evolution of the overlap among them. We expect that the system will show a  $P(q)$  peaked at a certain value up to a scale of time  $t_0$  which is the scale of time over which it was thermalized. For times greater than  $t_0$  it will begin to surmount energy barriers larger than those of order  $T \log(t_0)$  and the replicas will uncorrelate, feeling that over scales of time greater than  $t_0$  they were not yet thermalized. Our results for a sample of size  $L = 14$  are shown in figure 17. We have thermalized four pairs of two replicas down to

$T = 1.5$  over  $t_0 = 60\,000$  Monte Carlo steps and then we have computed the  $P(q)$  over four successive periods, each of 15 000 Monte Carlo steps. One can see that there is a peak centred in an overlap which moves from  $q_{\max} = 0.48$  in the first 15 000 Monte Carlo steps to  $q_{\max} = 0.466$  in the following 15 000. In the last period the pairs of replicas begin to uncorrelate and their trajectories in phase space begin to deviate. In some sense, the samples are in equilibrium over a scale of time equal to that over which they were thermalized. This is a characteristic of ageing phenomena, which are some of the most interesting behaviours in spin glasses.

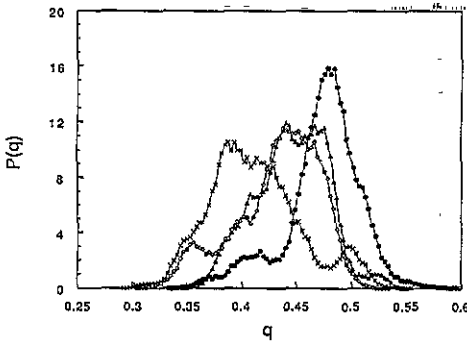


**Figure 17.**  $P(q)$  at  $T = 1.5$ ,  $L = 14$  over four successive periods of 15 000 Monte Carlo steps after  $t_0 = 60\,000$  initial steps of thermalization. ●, first period; Δ, second; ◇, third; ×, fourth.

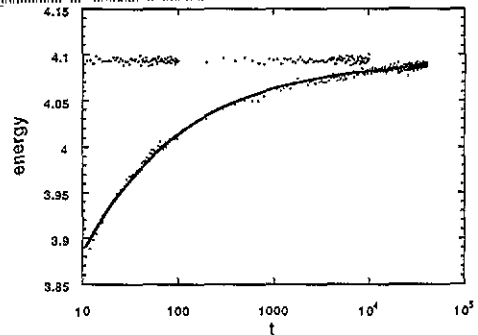


**Figure 18.** The energy as function of time, starting from a random configuration. The fit is of the form  $A + Bt^{-C}$  with  $C = 0.42$ . The horizontal line of points is the time evolution of the internal energy for thermalized configurations.

Now we show some results on the behaviour of the energy overlap. The existence of a discontinuity in  $q^e$  is a crucial prediction of broken replica theory and it is very important to have an independent verification of the existence of this discontinuity without having to rely on the extrapolation to  $\epsilon \rightarrow 0$  of equation (15).

To this end we have prepared a larger system (an  $18^4$  lattice) in two different ways such that the initial conditions at time zero constrain the system to stay in one of the phases which are obtained in the limiting procedure ( $\epsilon \rightarrow 0$ ), i.e.  $q = q_{\max}^e$  or  $q = q_{\min}^e$ . This approach, however, works well only for very large lattices and for times not so large that the tunnelling among different states of the system are not allowed. If the system is large the requirement on the time is normally satisfied, because the time needed for tunnelling increases exponentially with the size of the system.

In the first case we start from two different random configurations and we quench them at  $T = 1$ . We see a process of energy relaxation and the energy dependence as a function of the Monte Carlo time can be well fitted by a constant plus a corrective term that decreases like a power of time, as can be seen in figure 18.

In this case we expect that the system will evolve towards two different equilibrium states in each replica and that the two states will be not correlated. At zero magnetic field we therefore expect that the overlap among the two replicas is 0 and the energy overlap goes to  $q_{\min}^e$  for sufficiently large times. The data for  $q^e$  as a function of the Monte Carlo time, up to  $20 \times 10^6$  iterations, are shown in figure 19 and can be well fitted by a constant plus a corrective term that decreases like a power of time.

For the same system we have produced a well thermalized configuration of a single replica by a slow cooling procedure. We have put the two replicas in this configuration at

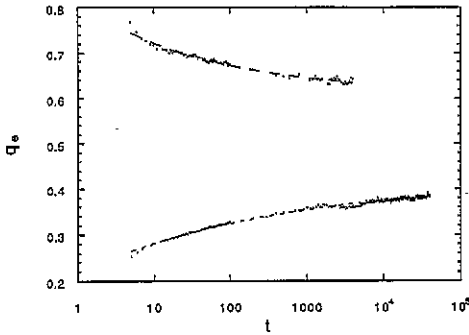


**Figure 19.** The energy overlap as function of time, starting from two random configurations (lower curve) and two identical equilibrium configuration (upper curve). The fits are of the form  $A+Bt^{-C}$  with  $A = 0.41$  and  $C = 0.17$  in the first case and  $A = 0.61$  and  $C = 0.27$  in the second case.

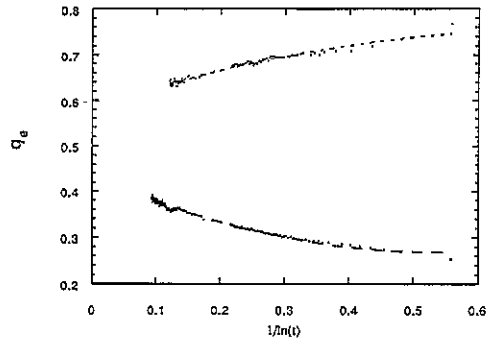


**Figure 20.** The same data as in figure 19 plotted versus  $1/\ln(t)$  and fitted with a polynomial of this variable. The values extrapolated at  $t = \infty$  are  $A = 0.43$  and  $A = 0.58$ , respectively.

time zero and have monitored the energy overlap. Here we must take measurements up to a time which is comparable with the thermalization time; otherwise (as we have commented previously in the case of the  $P(q)$ ) one may see some artefacts due to the fact that the starting configuration is not at perfect equilibrium. Here also the data for  $q^e$  as function of the Monte Carlo time, up to  $3 \times 10^6$  iterations, are shown in figure 19 and can be well fitted by a constant plus a corrective term that decreases like a power of time.

The asymptotic values extracted using this technique are not sensibly different and they are very similar to those obtained by the extrapolation to  $\epsilon \rightarrow 0$  in equation (15) (see [7]).

The suspicious reader may fear that a power-law extrapolation may give biased results and that the approach to equilibrium is slower. In order to remove these last doubts we have plotted the data versus  $1/\ln(t)$  and have fitted a polynomial of this last variable (see figure 20). Again assuming a very slow approach to equilibrium, the values of the minimum and maximum energy overlaps are different and very similar to those obtained with the power-law fit of figure 19.

These results are in agreement with finite-size scaling predictions for small samples shown in the previous sections and studies of very large ones [7]. Also they propose interesting tools to study large sizes which we are not able to thermalize and suggest that four-dimensional spin glasses thermalize in a complex landscape with many valleys, as happens in a wide variety of disordered systems with replica symmetry breaking features.

## 7. Conclusions

In this work we have shown some results which support the idea of a spin-glass phase in the four-dimensional Ising spin glass with replica symmetry breaking features. This work, complementing another in which equivalent results have been presented for very large samples and using different numerical procedures [7], tries to shed light on the nature of the spin-glass phase and presents numerical predictions which could aid in constructing a future spin-glass field theory. These techniques can also be used in other short-ranged models (especially at three dimensions) and to understand the nature of the phase transition of the four-dimensional Ising spin glass in a magnetic field [25].

We have studied the behaviour of the tail of the  $P(q)$  and we have found that it scales with size in a similar way to that at the critical point. In this way we are able to predict the values for some exponents even though we are not able to establish them with any accuracy. In order to obtain their values within the spin-glass phase and to study what type the singularity in the peak of the  $P(q)$  is, more refined numerical simulations with more samples (we studied a number of samples of order 100) and more statistics (we collected data over 20 000 Monte Carlo steps and this is not very much) are needed. We have also tested an interesting prediction using renormalization group arguments below six dimensions, i.e. the scaling of  $q(x)$  given by equation (20). This is in agreement with our data even though a more extensive study would be welcomed.

We have also studied the probability distribution of energy overlaps  $P(q^e)$ . We have found that it develops two peaks plus a continuous part (reminiscent of the  $P(q)$  for the SK model with a magnetic field). We are able to determine the maximum and minimum overlaps and the discontinuity  $q_{\max} - q_{\min}$  goes to zero at the critical point faster than does the overlap  $q_{\max}$ . This is consistent with  $de > 2dq$ . At the critical point the behaviour of the tail is dominated by regular terms and this changes within the spin-glass phase. We cannot say if this happens continuously or abruptly when the critical temperature is passed, even though the last possibility would seem the most natural.

Moreover, we have presented results on ultrametricity where possible violations of the triangular inequality have been excluded. Our results do not show this effect clearly, neither do they exclude it. To decide this question one should go to lower temperatures (for example, down to  $T = 0.5T_c$ ).

Finally we have presented some results for large samples on the tail of the  $P(q)$  which we hope is self-averaging and thermalizes in a time scale  $L^z$ ,  $z$  being a dynamical exponent. Then it should thermalize faster than the crossing among states which increases exponentially with size. We also showed results for the energy overlap  $q^e$  for a very large size ( $L = 18$ ) in the off-equilibrium regime which gives further support to the finite discontinuity of the energy overlap. This is in agreement with a replica broken phase. Our results give support to the idea of a complex structure of the phase space in the four-dimensional Ising spin glass. We suspect that some scaling laws will be also present when the thermalization takes a finite amount of time. This is not new and very interesting results have been already presented [23].

Finally, one could ask if some scaling law could be present in the continuous part of the  $P(q)$ . This is difficult because in that region one sees the superposition of several contributions coming from different pure states. Instead the tail explores the behaviour of one dominant state and, even though we expect some noise in the tail due to some states of the continuous part near the peak, we think that the effect of the state at  $q = q_{\max}$  will be prominent.

## Acknowledgments

FR is supported by the European Community and JCC is supported by DGA in Spain. JCC acknowledges CAI and COMA for their financial support while he stayed in Rome. Part of the simulations were performed in a Transputer machine of 64 nodes (T805) with a peak performance of 100 Mflops [24] whose construction has been funded by CNR in Italy.

## References

- [1] Mezard M, Parisi G and Virasoro M A 1987 *Spin Glass Theory and Beyond* (Singapore: World Scientific)
- [2] Binder K and Young A P *Rev. Mod. Phys.* **58** 801
- [3] Parisi G 1992 *Field Theory, Disorder and Simulations* (Singapore: World Scientific)
- [4] Sherrington D and Kirkpatrick S 1978 *Phys. Rev. B* **17** 4384
- [5] Mézard M, Parisi G, Sourlas N, Toulouse G and Virasoro M 1984 *J. Physique* **45** 843
- [6] Fisher D S and Huse D A 1988 *Phys. Rev. B* **38** 386
- [7] Parisi G and Ritort F 1993 *J. Phys. A: Math. Gen.* **26** 6711
- [8] Reger J D, Bhatt R N and Young A P 1990 *Phys. Rev. Lett.* **16** 1859
- [9] Grannan E R and Hetzel R E 1992 *Phys. Rev. Lett.* **67** 907
- [10] Badoni D, Ciria J C, Parisi G, Pech J, Ritort F and Ruiz J J 1993 *Europhys. Lett.* **21** 495
- [11] Caracciolo S, Parisi G, Patarnello S and Sourlas N 1990 *Europhys. Lett.* **11** 783
- [12] De Dominicis C, Kondor I and Temesvari T *Preprint SphT/92/079*
- [13] Parisi G and Virasoro M A 1989 *J. Physique* **50** 3317
- [14] Parisi G, Ritort F and Slanina F 1993 *J. Phys. A: Math. Gen.* **26** 3775
- [15] Franz S, Parisi G and Virasoro M A 1992 *J. Physique I* **2** 1869
- [16] De Dominicis C and Kondor I 1984 *J. Physique Lett.* **45** L-205
- [17] De Dominicis C and Kondor I 1985 *Lecture Notes in Physics* vol 216, ed L Garrido (Berlin: Springer)
- [18] De Dominicis C 1989 *J. Physique* **50** 2767
- [19] De Dominicis C and Kondor I 1990 *Physica A* **163** 265
- [20] Singh R R P and Chakravarty S 1986 *Phys. Rev. Lett.* **57** 245
- [21] Kondor I, De Dominicis C and Temesvari T *Preprint SphT/91/159*
- [22] Parisi G, Ritort F and Rubi J M 1991 *J. Phys. A: Math. Gen.* **24** 5307
- [23] Blundell R E, Humayun K and Bray A J 1992 *J. Phys. A: Math. Gen.* **25** L733
- [24] RTN collaboration 1992 *Experience on RTN (Proc. Int. Conf. on Computing in High Energy Physics '92 (Annecy))* (CERN) *Reconfigurable Transputer Network Technical Notes ROM2F/92/41* and University of Zaragoza
- [25] Ciria J C, Parisi G, Ritort F and Ruiz-Lorenzo J J 1994 *J. Physique II* (to appear)